

Hybrid fire detection using hidden Markov model and luminance map[☆]

Liqiang Wang^{*}, Mao Ye, Jian Ding, Yuanxiang Zhu

School of Computer Science and Engineering, University of Electronic Science and Technology of China, Chengdu 611731, PR China
State Key Lab for Novel Software Technology, Nanjing University, PR China

ARTICLE INFO

Article history:

Received 15 May 2010

Received in revised form 9 September 2011

Accepted 13 September 2011

Available online 22 October 2011

ABSTRACT

Recently, fire detection is a hot research topic. Although many detection methods have been proposed, there exist high false alarms because of the interference of fire-colored moving object in the complex environments. In this paper, a hybrid method is proposed. First, we get the set of candidate fire regions. Then these candidate fire regions are analyzed to exclude the fire-colored moving object. Our contributions are using the hidden Markov model (HMM) based on spatio-temporal feature and the variance of luminance map motivated by visual attention, and combining both for fire detection. The wrong detection can be reduced greatly. Experiment results show our proposed method has a good performance and it is robust to be used in complex environment compared with previous algorithms.

© 2011 Elsevier Ltd. All rights reserved.

1. Introduction

Fire is a kind of serious natural disasters, which causes huge losses to people's lives and properties. If it can be alarmed in advance, then this loss will be reduced greatly. Therefore, developing an effective and robust fire detection algorithm is very important. With the development of computer vision and pattern recognition, fire detection method based on intelligent video surveillance (IVS) has received more attention. Many methods were proposed by using fire features to construct models for fire detection [1–3]. Practically, detecting fire with the interference of various fire-colored moving objects is a great challenge. In this paper, we will propose a method to handle this critical problem.

Previous many works concentrated on constructing models, which make use of various visual features including color, motion and geometry of the fire regions. However, these models are not stable and have a high rate of false alarm because of the interference of fire colored object. The representative algorithms can be summarized as the following. Color clues were used for flame detection in [4]. Flame pixel colors and their temporal variations were used in [1]. A change detection scheme was utilized to detect flicker in the fire regions [2].

Fast Fourier transforms (FFT) of temporal object boundary pixels were computed to detect peaks in Fourier domain [5], because it is claimed that turbulent flames flicker with a characteristic flicker frequency of around 10 Hz is independent of the burning material [6,7]. The shapes of fire regions in Fourier domain was also studied in [8]. However, an important weakness of Fourier domain methods is that flame flicker is not purely sinusoidal but it's random in nature. As a result, there may not exist any peaks in FFT plots of the fire regions. In addition, Fourier transform does not have any time information. Therefore, short-time Fourier transform (STFT) can be used requiring a temporal analysis window. In this case, temporal window size becomes an important parameter for detection. If the window size is too long, one may not observe peakiness in the FFT data. If it is too short, one may completely miss cycles and therefore no peaks can be observed in the Fourier domain. A wavelet transform was used to analyze the flicker frequency feature of the flame in [9]. However, the performance

[☆] Reviews processed and approved for publication to the Editor-in-Chief Dr. Manu Malek.

^{*} Corresponding author at: School of Computer Science and Engineering, University of Electronic Science and Technology of China, Chengdu 611731, PR China.

E-mail addresses: cvlab.uestc@gmail.com, yem_mei29@hotmail.com (L. Wang).

depends on the real application scenes. A HMM model was used to detect flame flicker in [3,10,11], three hidden states are fire color pixels, non-fire pixels, looks like fire color pixels, but it cannot suit for complex outdoor scenes.

In this paper, we propose an algorithm using HMM based on spatio-temporal feature and variance of luminance map to improve the fire detection accuracy, which improves our previous algorithm in [12]. More theoretical analysis and thorough experiments are added. Our algorithm not only detects fire colored moving regions in video, but also analyzes both the motion of such regions in wavelet domain for flicker estimation and the variance of luminance map in temporal. In the first step of the algorithm, we get the set of candidate fire regions through moving object detection and color analysis. Then a HMM based on spatio-temporal feature will be constructed. At the same time the variance of luminance on the candidate fire regions is analyzed. Finally, a final conclusion will be drawn whether the candidate fire region is a true fire region.

2. Previous works

There are many methods for fire detection described in previous work [1–8,10,11,13]. Generally speaking, the recognition process is as the following: (1) detection of the moving regions; (2) detection of the fire-colored pixels; (3) removing the non-fire region from the set of candidate fire regions. In the second step, some non-fire colored moving objects will be excluded. At the final step, some fire-colored moving objects will be removed using some models on the set of candidate fire regions.

2.1. Moving object detection

Moving object detection is the basis of object recognition. There are two simple and efficient segmentation methods, which are “background subtraction” and “frame subtraction”, respectively. Here we adopt the “background subtraction” method, which can be realized easily and has a robust performance. It also meets the real-time application requirement.

In this paper, we use the method in [14] to separate moving pixels and background pixels. This method can easily separate moving objects and connected regions. Let $B_n[k, l]$ and $I_i[k, l]$ stand for the intensity values of background and current images at pixel position $[k, l]$ in the n th frame separately. The background intensity value $B_{n+1}[k, l]$ is computed as the following:

$$B_{n+1}[k, l] = \begin{cases} aB_n[k, l] + (1 - a)I_n[k, l], & \text{if } [k, l] \text{ is non-moving,} \\ B_n[k, l], & \text{if } [k, l] \text{ is moving,} \end{cases} \quad (1)$$

where the update parameter a is a positive real number between 0 and 1.

The moving pixels are estimated by subtracting background image from current image with a threshold. These pixels are grouped into connected regions (blobs) and labeled by a two-level connected component labeling algorithm [15].

2.2. Fire-colored pixel detection

In order to get the candidate fire regions, first, color analysis can be used to remove non-fire colored moving objects. There are several methods described in [2,9,10], which are widely used in applications. In this paper, we use the method in [2] whose main idea is that if the pixel value of moving region satisfies three condition formulas, it will be considered as a fire-colored pixel. The fire color model in [2] is used for defining the fire pixels. Although there are various types of fire, fire in the initial stages shows a color range from red to yellow. Considering RGB color-space, the inter-relation component of R , G and B color channels is as follows: $R > G > B$. Besides, the component of R should be the dominating color channel, so another condition is that R will be over a determined threshold R_T . However, light conditions in the background may have great influence on saturation values, which may cause non-fire pixels to be considered as fire pixels. All of conditions are summarized and described as the following:

$$\begin{cases} \text{Condition1 : } R > R_T, \\ \text{Condition2 : } R > G > B, \\ \text{Condition3 : } S > (255 - R)S_T/R_T, \end{cases}$$

where S_T is the value of saturation when the threshold of R channel is R_T . If the pixel in moving region satisfies these three conditions, it will be considered as a fire-colored pixel.

3. Our methods

Now, we have got the set of candidate fire regions. Then we will propose our algorithm to analyze these candidate fire regions for removing fire-colored moving objects. On the one hand, burning fire is flickering at a certain frequency around 10 Hz [10]. This flicker frequency is unique compared with most of other fire-color objects. If this predictable high-frequency behavior on the candidate fire regions can be detected, then we can remove most of non high-frequency fire-color objects

and the recognition will be more robust compared with the existing fire detection algorithms in [1–3,10,13,14]. In real application scenarios, the flame flicker frequency is not a constant and it varies on time. The variations of these flames are considered as a random event. Fortunately, HMM [16] is very suit for characterizing this random event.

We use HMM model based on spatio-temporal features to detect flame flicker process. The method can reduce most of false alarm in some scenarios, for example walking man with red-color clothes. On the other hand, the flying red-flag, which has high-frequency activity, will be hard to remove from the set of candidate fire regions. It can be observed easily that the burning flame is brighter than other background region and the luminance is varying overtime. Here, we use the luminance map to characterize temporal variance of luminance feature. Finally, after HMM and luminance map detection, a synthesized conclusion will be drawn. Fig. 1 shows the main process of our algorithm. All details will be introduced in the following subsections.

3.1. HMM model based on spatio-temporal features

In this section, we will introduce how to set observation points at first. Then the spatio-temporal features will be used to express the flame's flicker property. Here, a wavelet transform is used to measure the high-frequency variation of flame. At last, a HMM based on observation points will be used to judge whether the observation point is a fire point.

3.1.1. Setting observation points

As described in previous works [3,10], real flame has special temporal variance information such as turbulent flicker. That is to say, we can use an appropriate model to characterize the flicker behavior. HMM is fit for characterizing the random event. In this paper, we propose a HMM model based on spatio-temporal features to characterize the flame flicker. In this HMM, a group of observation points will be set around flame's boundary, because the flicker around the flame boundary is more obvious than other areas.

In previous works described in [3,10], a method based on fixed observation point at the boundary of flame was proposed to detect the flicker process. However, in real fire scenarios, flames of burning fire become irregular and turbulent growing. Because of airflow and noises in different environments, especially in outdoor scenes such as forest and public area, fixed observation point has its limitation. If we continue to use fixed observation point to detect flicker, the accuracy will decrease because the fixed observation point may be not in fire region.

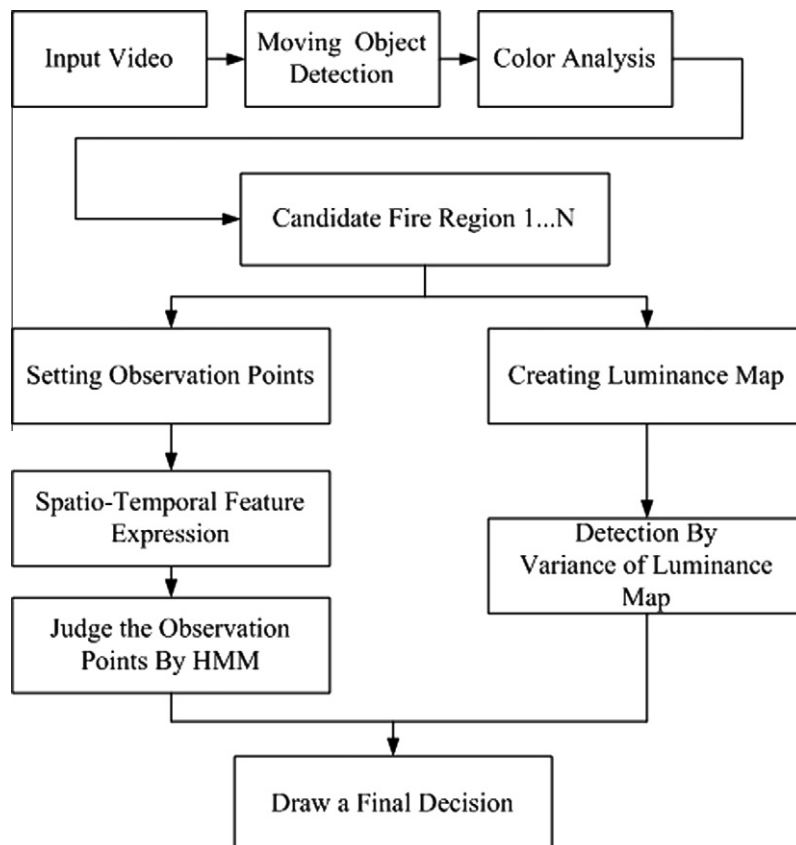


Fig. 1. The main process of our algorithm.

We hope that a group of observation points will be set automatically, so we can use multiple points together to improve the accuracy of fire detection. The method described in [17] helps us to find observation points around flame boundary automatically.

3.1.2. Spatio-temporal features

In order to improve the accuracy of fire detection, we need to find appropriate features to get a group of observation vectors. These vectors are used to construct observation probabilities with respect to hidden states. In our method, the observation vector is derived from spatio-temporal feature. Fig. 2 shows the spatio-temporal features on a frame picture. A channel C is divided into some cuboid to represent the local spatio-temporal observation values, where w , h , and l represent the width, height and length of the cuboid, respectively. This setting can reduce the loss of information around flame.

The values of a channel are derived by temporal wavelet transform [18] on the candidate fire region. In a two-channel wavelet decomposition, the parameters $\{-\frac{1}{4}, \frac{1}{2}, -\frac{1}{4}\}$ and $\{\frac{1}{4}, \frac{1}{2}, \frac{1}{4}\}$ are used for high-pass and low-pass filter coefficients, respectively. Here, we only use the high-frequency part after a two dimensional wavelet decomposition of the sample channel. The length of observation sequence is 20, Fig. 3 shows the values of observation samples after wavelet transform. The values are results of the observation points around a burning flame. The positive and negative values in this sequence are logically the same for modeling the changes in the channel. We only use the absolute value of them to obtain the final observation sequence. It can be observed easily that the values of the observation point fluctuate between the minimum and maximum values. By the way, in the following subsections, observation sequences $O_i(t = 1, 2, \dots, T; i = 1, 2, \dots, N)$ of this kind will be applied to HMM. Here, $i = 1, 2, \dots, N$ on behalf of the observation points, and each observation point has T observation values.

3.1.3. HMM model based on observation points

In [3,10], the authors fix a single observation point to set a one-dimensional signal representing the temporal variations, and three hidden states are derived by using threshold manually. While in our algorithm, the hidden states are got by adapting k -means algorithm at an abstract manner on $N \times T$ observation values. We use a new clustering algorithm described in [19]. After clustering, we construct a prototype of three-hidden states. The three states are high-frequency state, medium-frequency state and low-frequency state. Fig. 4 shows the three-hidden states' relationship. They are determined by spatio-temporal features of $N \times T$ training samples. It is difficult to depict the statistic character within each abstract hidden state, so a mixture of Gaussian (MOG) is used to approximately estimate the emission probabilities of each state. The emission probabilities of each state are illustrated as the following:

$$b_j(G) = \sum_{m=1}^M B_{jm} N'(G; \mu_{jm}, \sigma_{jm}), \quad j = 1, 2, 3 \quad (2)$$

where M is the number of Gaussian distribution, N' is the Gaussian pdf and G is the observation space. The mean for the m th Gaussian at state j is μ_{jm} , while σ_{jm} is the variance for it. The values of these two variables can be figured out through the k -means clustering, which is well detailed in [19].

In the former steps, we have obtained the observation values. In tractional HMM, there are 5 parameters $\lambda = \{\pi_i, A_{ij}, B_{j,m}, \mu_{jm}, \sigma_{jm}\}$, where π_i is initial state probabilities, A_{ij} is the transition probability from state i to j , and $B_{j,m}$ is the mixture parameters for MOG. A certain HMM is established by training these parameters by a series of observation

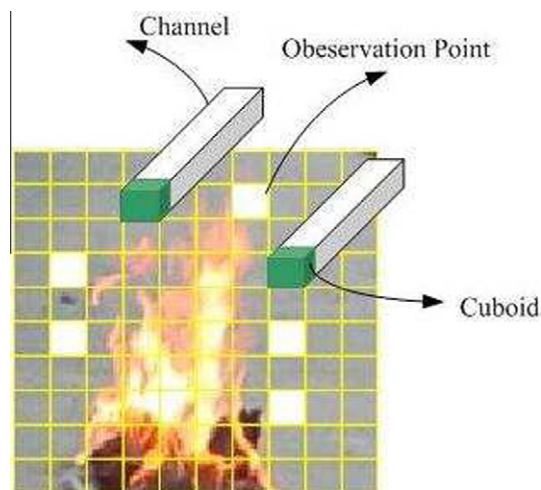


Fig. 2. The spatio-temporal features and observation points.

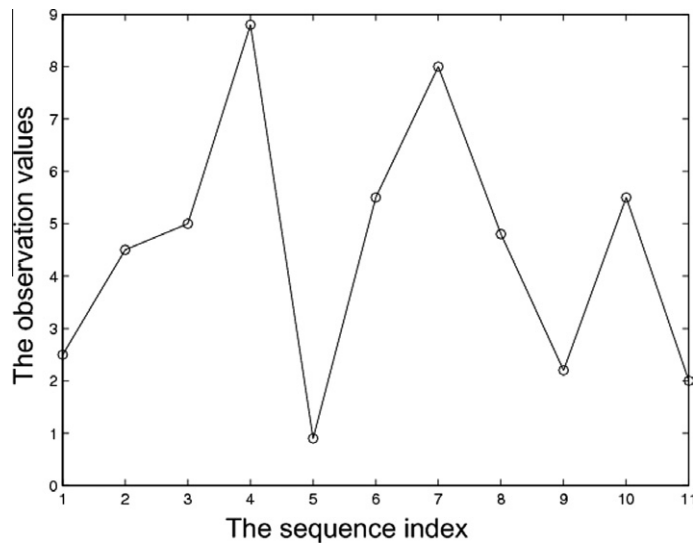


Fig. 3. Observation point's values after temporal wavelet transform.

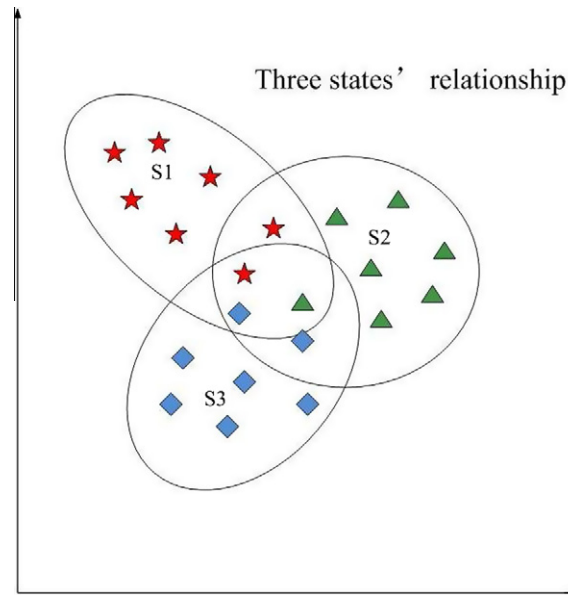


Fig. 4. Three hidden states.

sequences $O_t^i (t = 1, 2, \dots, T; i = 1, 2, \dots, N)$, where $i = 1, 2, \dots, N$. Generally, expectation maximization (EM) algorithm is widely used for HMM parameter-estimation, but it exists some local minimums in the process of iteration. In this paper we use a new method to initialize the parameters of λ . The μ_{jm} and σ_{jm} are derived by k -means clustering, and now we compute the former three parameters.

Here, we have $N \times T$ observation values for obtaining hidden states by clustering. Moreover, after k -means clustering, the $N \times T$ observation values will cluster into $3M$ classes with M for each state. Let $w_{i,k} (i = 1, 2, 3; k = 1, 2, \dots, M)$ stand for the number of samples clustered into the m th Gaussian of the j th state, then

$$B_{jm} = \frac{w_{i,k}}{\sum_{k=1}^M w_{i,k}} \quad (i = 1, 2, 3; k = 1, 2, \dots, M). \quad (3)$$

We can obtain $\{S_1(i); S_2(i); \dots, S_T(i)\} (i = 1, 2, \dots, N)$ given any observation sequences $O_t^i (t = 1, 2, \dots, T; i = 1, 2, \dots, N)$, where $\{S_1(i); S_2(i); \dots, S_T(i)\}$ is the hidden state sequence of the i observation point. Then we can initialize parameters π_i and $A_{i,j}$ based on the following formula,

$$\pi_i = \frac{\varepsilon_i}{N}, \quad i = 1, 2, 3 \quad (4)$$

where ε_i is the number of state s_i as the initial state in N sample sequences, and

$$A_{ij} = \frac{\alpha_{ij}}{\sum_{s=1}^3 \alpha_{is}}, \quad i, j = 1, 2, 3 \quad (5)$$

where α_{ij} is the times from state i to state j .

Through former steps, our algorithm appropriately initializes the HMM parameters. Then we can get the HMM parameters of the fire model through the iterations of EM algorithm. Based on these HMM parameters, we can preliminary judge the candidate fire region is a true fire region or not. Although it may exists some false alarms, many kinds of false alarm can also be removed. The max observation probability is evaluated by the forward-backward algorithms [20]. In order to illustrate the problem, we used the following Log likelihood form,

$$P = \ln(P(O_1(i), \dots, O_T(i)|\lambda)), \quad i = 1, 2, \dots, N. \quad (6)$$

If the value P is greater than \hat{P} , we can say that the i th observation point around the flame boundary is a fire point, where \hat{P} is a threshold, which is got empirically.

3.2. Temporal luminance map

Although HMM algorithm can remove most of fire-colored objects, the high-frequency fire-colored objects such as the flying red flag, will be hard to remove from candidate fire region only relying on flicker feature. In fact, it can be observed easily that the burning fire is brighter than other backgrounds. Here, we use an appropriate manner to characterize the variance of luminance feature. The main process is the following. Firstly, a luminance map will be created by center-surround difference operation. The center-surround difference operation helps us find the luminance salient region. Then, once the salient region is found, a threshold based on experiments will be used for the luminance map. In fact, the fire-colored objects with high-frequency luminance variance will not be fierce as true fire, the threshold in this method also can exclude the interference of fire-colored objects with high-frequency activity.

3.2.1. Creating luminance map

In order to create luminance map, the center-surround difference algorithm in [21] is used. The aim of center-surround difference algorithm is to give prominence for the luminance salient area [22] of an original input image. In the first, for the purpose of strengthen the edge of salient region, Gaussian pyramid [23] is used. For any input image $I_{m \times n}$, let the function $lpfilter$ stand for the low-pass filter, function $subsample(I) = I(1:2:m, 1:2:n)$, where the term $\{1:2:m\} = \{1, 3, 5, \dots\}$, $\{1:2:n\} = \{1, 3, 5, \dots\}$. We obtain I_1, I_2, \dots, I_6 from I by the following equation,

$$I_{i+1} = subsample(lpfilter(I_i)), \quad (i = 0, 1, \dots, 5),$$

where the horizontal and vertical image-reduction factors range from 1:1 (scale zero) to 1:6 (scale six). Then, a subtraction operation between $I_c(x, y)$ and $I_s(x, y)$ will get the difference map D_i as the following equation. D_i describes the edge of salient region,

$$D_i \equiv I_{c,s}(x, y) = |I_c(x, y) - I_s(x, y)|, \quad (i = 1, 2, \dots, 6) \quad (7)$$

where $I_c(x, y)$ is the center area's pixel value and the $I_s(x, y)$ is the pixel value of surrounding corresponding area. The center is a pixel at scale $c \in \{1, 2, 3\}$. While the surround is the corresponding pixel at scale $s = c + \delta$, $\delta \in \{2, 3\}$. Here, I_s should be interpolated to the size of I_c so that we can compute the differences of pixels. The 6 difference maps are

$$\begin{aligned} D_1 &= I_{1,3}, & D_2 &= I_{1,4}, \\ D_3 &= I_{2,4}, & D_4 &= I_{2,5}, \\ D_5 &= I_{3,5}, & D_6 &= I_{3,6}. \end{aligned} \quad (8)$$

Then, we normalize each D_i to N_i by following equation so that the feature value is between 0 and 1.

$$N_i(x, y) = \{D_i(x, y) - d_{min}\} / (d_{max} - d_{min}), \quad (i = 1, 2, \dots, 6) \quad (9)$$

where d_{max} and d_{min} represent the maximum and minimum values of D_i , respectively. Each N_i is interpolated to obtain the feature map F_i . In order to find the salient area, we compute the local standard deviations σ_j in $BLOCK(j)$ by the following operations,

$$\begin{aligned} \mu_j &= Mean(BLOCK(j)), \quad (j = 1, 2, 3, 4) \\ \sigma_j^2 &= Var(BLOCK(j)), \\ \sigma_{nj} &= \sigma_j / 255, \end{aligned}$$

where $BLOCK(j)$ are the four equal division regions from original input image. There are great difference of image characteristic in each region. The $\sigma_{n,j}$ is the normalized standard deviation.

After get the local standard deviations, we obtain binary image B_i from F_i as the following:

$$t_j = w_i \times \sigma_{n,j},$$

$$B_i(x, y) = \begin{cases} 1, & \text{if } F_{ij}(x, y) \geq t_j, \\ 0, & \text{otherwise} \end{cases} \quad (10)$$

where w_i is the weighting coefficient. Then an OR operation (11) is used to strengthen the salient region,

$$B(x, y) = \text{BinaryOR}\{B_i(x, y)\} \quad i = 1, 2, \dots, 6. \quad (11)$$

The location with binary 1 in $B(x, y)$ is the salient region of the input image. According to real application scene, the large binary objects [24] in salient map B may be background with high probability. So they should be removed as follows:

$$B_i(x, y) = 0, \quad \text{if } (\text{Area}(B_i(x, y))) > 2 \times T$$

where T is the maximum target size based on a prior knowledge. At last, the weight w_i will be iteratively changed by Eq. (12) unless the number of salient regions is greater than T_0 or w_i is less than w_{th} ,

$$w_{i+1} = w_i - \varepsilon. \quad (12)$$

By the way, during the algorithm, the following parameters ε , T_0 , w_0 and w_{th} should be specified. They are iteration difference value, the number of salient regions, initial weight coefficient and threshold of w_i , respectively. After a series of former operations, the salient area will stand out. Fig. 5 shows the result of center-surround difference operation, but the defect is the noise interference.

Considering our application field, we improve the center-surround difference algorithm. As the complex environment has much of noise interference, we compute more local region deviations to amend the threshold t_j . We divide the original input image into 16 regions to compute the standard local standard deviations σ_j . After get the coarse luminance salient map, a group of morphology operations such as dilate and erode will be used to the coarse luminance salient map. After that operation, the noise interference can be reduced efficiently. Here we use the parameters $\varepsilon = 0.4$, $T_0 = 80$, $w_{th} = 4.0$ and initial value of $w_0 = 5.2$ in our experiment. Fig. 6 shows the result of our improved center-surround difference operation. We successfully find the luminance salient region with less noise interference.

3.2.2. The variance of luminance map

After previous operations, we have created the luminance map. The variance of luminance map is implemented by characterizing the temporal luminance changes on the candidate fire region through consecutive several frames. Here we use Eq. (13) to get the variance of luminance map of a pixel (x, y) in consecutive 10 frames,

$$v = \sum_{\tau=1}^{10} |S_{x,y}(\tau) - S_{x,y}(\tau + 1)|, \quad (13)$$

where $S_{x,y}(\tau)$ is the value of a pixel (x, y) in consecutive 10 frames of the binary salient map B . Assuming that a pixel is included in a fire region, the variance of luminance will increase because of turbulent character of burning fire. Then we can set a threshold based on experiments. If the variance of a pixel v is lower than the threshold v_{th} , it will be removed from the set of candidate fire regions. On the other hand, suppose that a pixel is included in the high-frequency colored moving object, the variance of luminance v will not change frequently as the true fire region. The experiment results also prove this.

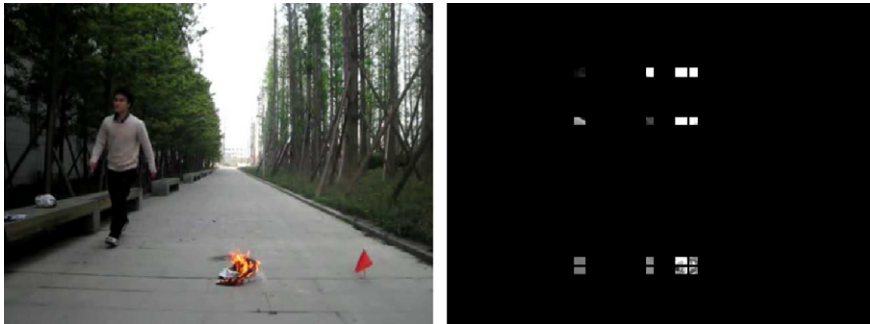


Fig. 5. Left picture shows the original input image. Right picture shows the result of using “center-surround difference” operation.



Fig. 6. Left picture shows the original input image. Right picture shows the result of using our improved center-surround difference operation. The noise is removed effectively.

4. Final decision

Our algorithm mainly analyzes the candidate fire regions. In the former steps, the HMM based on spatio-temporal feature detects the flicker and the variance of temporal luminance map analyzes the luminance changes. By above analysis, the suspected fire region without high-frequency red moving objects can be excluded by the HMM detection, while the suspected fire with high-frequency red moving objects can be excluded by analyzing the variance of luminance map. Now, we combine both to draw a synthesized conclusion whether the candidate fire region is true fire region.

In total detection process, we use the decision mechanism based on thresholds. The thresholds for computing the candidate fire regions are used to exclude non-fire colored moving objects. In the HMM detection process, true fire's flicker frequency is greater than that of normal fire-colored moving objects, so the thresholds based on experiments can distinguish true fire from normal fire-colored moving objects. During the luminance map detection, the variance of luminance map in true fire is greater than suspected fire, the fire-colored moving objects which have high frequency through threshold can be excluded. So the thresholds in the paper play a role of "justice". In the final decision, if the pixels of the candidate region satisfy the conditions of fire's HMM and the variance of luminance map, this region will be recognized as a true fire region in the end. Otherwise, it will be removed from the set of candidate fire regions.

5. Experiment results and analysis

In this section, we will show the experiments and analyze the results. In the part 1 experiments, we compare the method only using moving object detection and color analysis (Method 1) with our method only using HMM based on spatio-temporal feature (Method 2). In the following video, see Fig. 7 the walking man with red coat will cause false alarm using Method 1, while this false alarm can be removed by Method 2. Because Method 2 detects the flicker of the observation points which are set around the boundary of the flame automatically, while the walking man with red coat does not have the flicker feature. However, the flying red-flag which has high-frequency fire-colored object cannot be excluded from the candidate fire region sets. These moving objects have similar flicker feature as that of true fire.

In the part 2 experiments, we get the luminance map of the fire picture. We successfully found the salient regions in the fire picture by our improved center-surround difference operation. The luminance variance of red-flag is not obvious compared with true fire. Through analyzing the variance of luminance, fire-colored object with a high-frequency activity, such as red-flag, can be removed. The result of the second part experiment is shown in Fig. 8.



Fig. 7. Left picture shows the result only using moving object detect and color analysis. Right picture shows the result of previous work using HMM Model to detect the flame's flicker of burning fire.



Fig. 8. Left picture shows the original image. Right picture shows the result of using the variance of luminance map analysis. The red-flag is removed successfully. (For interpretation of the references to colour in this figure legend, the reader is referred to the web version of this article.)

In the part 3 experiment, we combine the HMM based on spatio-temporal feature and the variance of temporal luminance analysis to detect fire. Here the HMM is used by setting observation points around the boundary of fire, while the variance of temporal luminance is used by constructing luminance map. Our proposed algorithm not only detect the motion and color feature, but also detect the flicker and luminance change feature. So our method can remove not only the popular fire-colored moving objects like the people with red coat, but also fire-colored objects with a high-frequency activity, such as the red-flag. In the following video, see Fig. 9 we compare our method which only detects flicker with our hybrid algorithm.

Now, a group of fire videos in real-life complex environments will be detected by our proposed hybrid algorithm. They are refinery fire, fire fighters start a controlled brush fire, house fire with live sparking wire and vehicles fire. These public free videos are come from <http://www.ultimatechase.com/>. In the first scene, there are much smoke interference. In the second scene, the people with red clothes and the wind will have great influence on the recognition result. In the third scene, the sparking also will have great interference on the recognition result. In the last scene, the smoke and the wind will disturb the recognition. However, the four kinds of fire are detected successfully in time by our proposed algorithm, and the results have very low rate of false alarm and omission alarm.

At last, we evaluate the performance among our proposed hybrid method and other major methods with 30 videos. The 30 videos are divided into three categories of main scenes. Scene 1 only has fire. Scene 2 has fire-colored object interference without high-frequency activity. The last kind of scene has popular fire-colored objects and other fire-colored objects with a high-frequency activity. Each scene includes 10 videos. The recognition results on these three kinds of scenes using our proposed hybrid algorithm and other main methods are shown in Table 1 and Fig. 10. All experiment results prove that our algorithm is robust and has less false alarm and omission alarm compared with other methods.



Fig. 9. Left picture shows the result of our proposed method only using HMM to detect flame's flicker of burning fire. Right picture shows the result of our proposed hybrid algorithm.

Table 1

Our proposed algorithm compared with the previous algorithms on omission alarms and false alarms in the three kinds of scenes.

Method	False alarms			Omission alarms		
	Scene 1	Scene 2	Scene 3	Scene 1	Scene 2	Scene 3
Motion and color analysis only	3	7	9	3	4	6
Previous algorithms using HMM	2	4	6	2	3	4
Our algorithm only using HMM	1	3	4	2	2	2
Our proposed algorithm	0	1	1	0	1	1

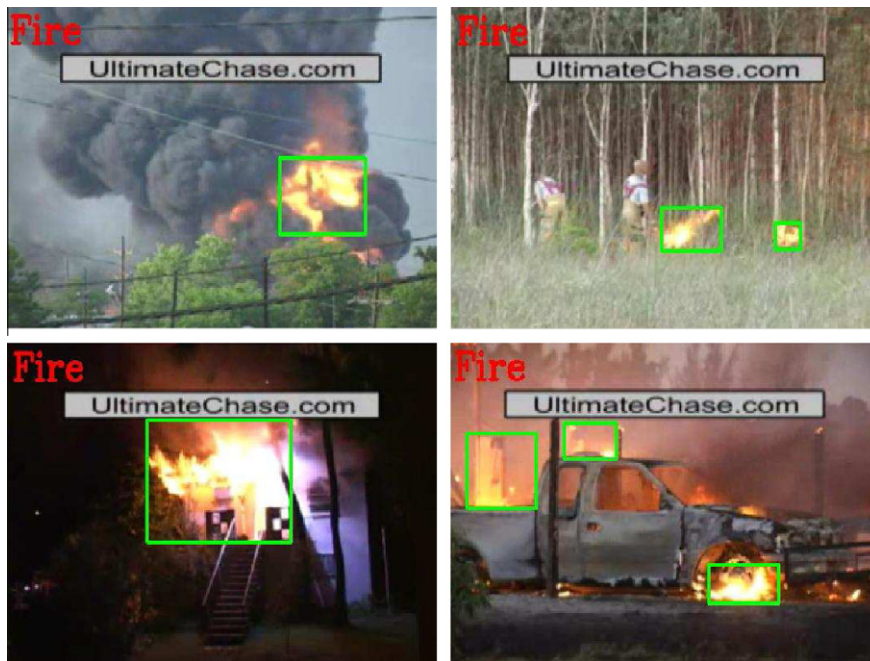


Fig. 10. The four pictures show the results of our proposed hybrid algorithm. They are refinery fire, forest fire, house fire and vehicles fire from left to right, which are all recognized successfully.

6. Conclusion

There exist many algorithms for fire detection, the detection accuracies have great differences. Through our analysis, fire has two kinds of features, static features and dynamic features. Static features are color and texture. Dynamic features are flicker and variance of luminance and so on. Many papers have mentioned these two kinds of features. In our opinion, if we want to improve the accuracy of fire detection, efficient feature should be found to characterize the fire, and the appropriate model is used to express the efficient features. In this paper, we proposed a hybrid method using HMM based on spatio-temporal feature and the variance of luminance based on visual attention to detect the fire. At first, we get the candidate fire region by moving object detection and color analysis. Then we focus on the candidate fire region analysis. On the one hand, the HMM based on spatio-temporal feature characterizes the flicker feature of burning fire, and a series of observation points have been set on the boundary of flame to judge the fire flicker feature. On the other hand, the variance of luminance map based on visual attention characterizes the temporal luminance feature. Here, in the hybrid detection algorithm, we use the layer filtering mechanisms for fire detection so that it can exclude most of fire-colored moving objects interference. Since our algorithm can reduce false alarms and omission alarms efficiently compared with previous algorithms. It is proved that our proposed method is robust and adapt to complex outdoor environment by a great of practical application scenario detection. In the future, we will analyze the texture in graphic field to further improve the accuracy of recognition.

Acknowledgments

This work is supported in part by the National Natural Science Foundation of China (60702071), 973 National Basic Research Program of China (2010CB732501), Foundation of Sichuan Excellent Young Talents (09ZQ026-035) and Open Project of State Key Lab for Novel Software Technology of Nanjing University.

References

- [1] Phillips III W, Shah M, Lobo NV. Flame recognition in video. *Pattern Recognit Lett* 2002;319–27.
- [2] Chen T, Wu P, Chiou Y. An early fire-detection method based on image processing. In: *Proceedings of the IEEE international conference on image processing (ICIP)*, 2004. p. 1707–10.
- [3] Toreyin BU, Dedeoglu Y, Cetin AE. Flame detection in video using hidden Markov models. *ICIP '05* 2005;2(2):1230–3.
- [4] Healey G, Slater D, Lin T, Drda B, Goedeke AD. A system for real-time fire detection. In: *Proceedings of the IEEE conference on computer vision and pattern recognition (CVPR)*, 1993. p. 15–17.
- [5] Rizzotti D, Schibli N, Straumann W. Method and device for detecting fires based on image analysis. *European Patent* 2002. EP 1364-351.
- [6] Albers BW, Agrawal Ajay K. Schlieren analysis of an oscillating gas-jet diffusion. *Combust Flame* 1999;119(1–2):84–94.
- [7] Chamberlin DS, Rose A. The flicker of luminous flames. In: *Proceedings of the symposium on combustion*, vol. 1–2, 1948. p. 27–32.
- [8] Liu CB, Ahuja N. Vision based fire detection. In: *The 17th international conference on pattern recognition ICPR'04*, vol. 4, 2004.

- [9] Toreyin BU, Dedeoglu Y, Cetin AE. Wavelet based real-time smoke detection in video. EUSIPCO 2005;05.
- [10] Gunay O, Tasdemir K, Toreyin BU, Cetin AE. Fire detection in video using LMS based active learning. Fire Technol 2010;46(3):551–7.
- [11] Toreyin BU, Dedeoglu Y, Cetin AE. Real-time fire and flame detection in video. ICASSP 2005;05:669–72.
- [12] Wang LQ, Ye M, Zhu YX. A hybrid fire detection using hidden Markov model and luminance map. In: The 1st international conference on medical image analysis and clinical applications (MIACA 2010), 2010. p. 118–22.
- [13] Lai CL, Yang JC. Advanced real time fire detection in video surveillance system. ISCAS 2008;18(21):3542–5.
- [14] Collins RT, Lipton A, Kanade T, Fujiyoshi H. A system for video surveillance and monitoring. In: Proceedings of the American Nuclear Society (ANS) eighth international topical meeting on robotics and remote system, 1999. p. 25–9.
- [15] Heijden FV. Image based measurement systems: object recognition and parameter estimation. New York: Wiley; 1996.
- [16] Hayakawa H, Shibata T. Block-matching-based motion field generation utilizing directional edge displacement. Comput Elect Eng 2010;36(4):617–25.
- [17] Ke Y, Sukthanker R. PCA-SIFT: a more distinctive representation for local image descriptors. CVPR 04 2004;2:506–13.
- [18] Lu W, Sun W, Lu HT. Robust watermarking based on DWT and nonnegative matrix factorization. Comput Elect Eng 2009;35(1):183–8.
- [19] Bishop CM. Pattern recognition and machine learning. Springer Publisher; 2006.
- [20] Rabiner LR. A tutorial on hidden Markov models and selected application in speech recognition. Proc IEEE 1989;77(2):257–86.
- [21] Sun SG, wak DM. Automatic detection of targets using center-surround difference and local thresholding. Image and signal processing and analysis. ISPA; 2005.
- [22] Itti L, Koch C, Niebur E. Model of saliency-based visual attention for rapid scene analysis. IEEE Trans Pattern Anal Mach Intell 1998;20(11):1254–9.
- [23] Burt J, Adelson EH. The Laplacian pyramid as a compact image code. IEEE Trans Commun 1983;31(4):532–40.
- [24] Jain K. Fundamentals of digital image processing. Prentice Hall; 2003.

Liqiang Wang received the B.S. degree from China Three Gorges University, Wanzhou, China, in 2008 and M.Eng. degree from University of Electronic Science and Technology of China, Chengdu, China, in 2011. He is currently an research engineer in the company XunLei. His research interests includes computer vision and machine learning.

Mao Ye received the Ph.D. degree in mathematics from Chinese University of Hong Kong, in 2002. He is currently a professor and Director of CVLab at UESTC. His current research interests include machine learning and computer vision. In these areas, he has published over 70 papers in leading international journals or conference proceedings.

Jian Ding received the B.S. degree in mathematics from Southwest University, Chongqing, China, in 2009. He is currently a postgraduate student in University of Electronic Science and Technology of China, Chengdu, China. His current research interests include abnormal behavior detection and analysis, cloth searching in computer vision.

Yuanxiang Zhu received the M.S. degree in computer science from Zhejiang University, Zhejiang, China, in 2002. He is currently a Ph.D. student in University of Electronic Science and Technology of China, Chengdu, China. His current research interests include machine learning and computer vision.